J., Ed.; Academic: London, 1984; p 77. (c) Sawamoto, M.; Miyamoto, M.; Higashimura, T. *Ibid.* p 89. (d) Higashimura, T.; Sawamoto, M. *Makromol. Chem., Suppl.* **1985**, *12*, 153. (e) Sawamoto, M.; Higashimura, T. *Makromol. Chem., Macromol. Symp.* **1986**, *3*, 83. (f) Higashimura, T.; Aoshima, S.; Sawamoto, M. *Ibid.* **1986**, *3*, 99.
(5) Higashimura, T.; Tanizaki, A.; Sawamoto, M. *J. Polym. Sci., Polym. Chem. Ed.* **1984**, *22*, 3173.
(6) Higashimura, T.; Miyamoto, M.; Sawamoto, M. *Macromolecules* **1985**, *18*, 611.
(7) Oya, S.; Sawamoto, M.; Higashimura, T. *Polym. Prepr., Jpn.* **1983**, *32*, 190, and another paper to be published.
(8) Tanizaki, A.; Sawamoto, M.; Higashimura, T. *J. Polym. Sci., Polym. Chem. Ed.* **1986**, *24*, 87.
(9) For suppression of chain transfer and termination, a principle ("quasi-living polymerization") that differs from ours has been proposed: Kennedy, J. P.; Kelen, T.; Tüdös, T. *J. Macromol. Sci., Chem.* **1982-1983**, *A18*, 1189 and the papers included in the same issue.
(10) In addition to these three systems, recent papers report new initiators, consisting of a metal halide and a carboxylic acid ester, for living cationic polymerizations of isobutylene[10a,b] and vinyl ethers:[10c] (a) Faust, R.; Kennedy, J. P. *Polym. Bull. (Berlin)* **1986**, *15*, 317. (b) Nagy, A.; Faust, R.; Kennedy, J. P. *Ibid.* **1986**, *15*, 411. (c) Aoshima, S.; Higashimura, T. *Ibid.* **1986**, *15*, 417.

Synthesis and Characterization of Vesicles Stabilized by Polymerization of Isocyano Functions

M. F. M. Roks,[1a] R. S. Dezentjé,[1a] V. E. M. Kaats-Richters,[1a] W. Drenth,[1a] A. J. Verkleij,[1b] and R. J. M. Nolte*[1a]

Laboratory of Organic Chemistry and Institute of Molecular Biology, University at Utrecht, 3584 CH Utrecht, The Netherlands. *Received September 5, 1986*

ABSTRACT: Coupling of dimethylhexadecyl(11-hydroxyundecyl)ammonium bromide with the *N*-formyl derivatives of L-alanine and L-valine and dehydration of the reaction products with phosphorus oxychloride and base yield the double-chain quaternary ammonium surfactants **1** and **2**, respectively. Via a similar sequence of reactions, starting from (*N*-formylamino)caproic acid and dimethyleicosyl- and dimethyldocosyl(11-hydroxyundecyl)ammonium bromide, the surfactants **3** and **4** are obtained. Amphiphiles **1-4** contain polymerizable isocyano functions located at different positions along the hydrocarbon chains. On dispersing in water these compounds form vesicles. Freeze-fracture electron microscopy and osmotic experiments indicate that the structures of the aggregates are closed. According to differential scanning calorimetry measurements the vesicles undergo a phase transition in the temperature range of -3 to -22 °C. Addition of nickel capronate to the vesicle dispersions results in polymerization of the isocyano functions in the bilayers. This polymerization proceeds more effectively for the isocyano functions at the end of the hydrocarbon chains than for the isocyano functions located in the middle section. The molecular weights vary between ~8000 and 45 000. Electron micrographs indicate that in vesicles of **3** and **4** the polymerization process is restricted to each of the monolayers. In **1** and **2** this process also includes the bilayer. Osmotic experiments and electron micrographs indicate that on polymerization the structure of the vesicles is retained, but the phase transitions disappear. Fluorescence experiments with the probes 8-anilino-1-naphthalenesulfonate and *N*-phenyl-1-naphthylamine reveal that the bilayers of the polymerized vesicles are less polar than those of the unpolymerized ones. This is the case for both the head-group region and the core of the bilayer matrix. From fluorescence isotope experiments in water and in D_2O we infer that in the polymerized vesicles the lower polarity of the head-group region is due to the extrusion of water molecules. The lower polarity of the core is probably correlated to the disappearance of the isocyano functions. Fluorescence experiments with the viscosity probe pyrene and fluorescence depolarization experiments with the probe 1,6-diphenyl-1,3,5-hexatriene suggest that on polymerization the bilayers of the vesicles become more viscous. On going from **1** to **4** the difference in fluorescence anisotropy values between polymerized and unpolymerized vesicles becomes smaller. This trend in declining difference of anisotropy values parallels the trend of decreasing molecular weight in polymerized **1-4**. For comparison fluorescence data are also included of experiments with vesicle systems prepared from dihexadecyldimethylammonium bromide, dioctadecyldimethylammonium bromide, egg yolk lecithin, dipalmitoylphosphatidylcholine, and a polymerizable methacrylate amphiphile.

Introduction

Phospholipids and double-chain synthetic surfactants form closed bilayer structures in water, known as liposomes and surfactant vesicles, respectively.[1] Because of their structural similarity to biological membranes, these aggregates are now widely being used in membrane mimetic studies.[2] In addition, these systems are of current interest as they could be applicable as devices for photochemical energy conversion,[3] slow release of drugs,[4] and as microreactors.[5] A drawback of liposomes and surfactant vesicles, however, is their limited stability, which obstructs their use in practical applications. In order to overcome this problem, several research groups have recently prepared polymerized vesicles from amphiphiles that contain diacetylene, butadiene, methacrylate, styrene, vinyl, thiol, amino acid, and isocyano groups.[6] A prerequisite for the exploitation of these systems is a good characterization of the structure of the polymerized aggregates. Detailed information can be obtained by applying the fluorescent probe technique. This technique has already been proved useful in studies of the structure and function of biological membranes in vivo.[7] Compared to other methods, such as EPR and NMR, the advantages are high sensitivity, low degree of membrane perturbation, and primary response to the environment.[7,8] The fluorescent probe technique has also been applied for the characterization of liposomes, enzymes, micellar systems,[8] and, more recently, synthetic surfactant vesicles.[9] Only a few reports deal with polymerized vesicle systems. Nome et al. studied the influence of vesicle polymerization on the fluorescence of pyranine.[10] They found that polymerization induces the formation of clefts on the vesicle surface.

In this paper, we describe the synthesis and characterization by fluorescence methods of unpolymerized and

0024-9297/87/2220-0920$01.50/0

Chart I

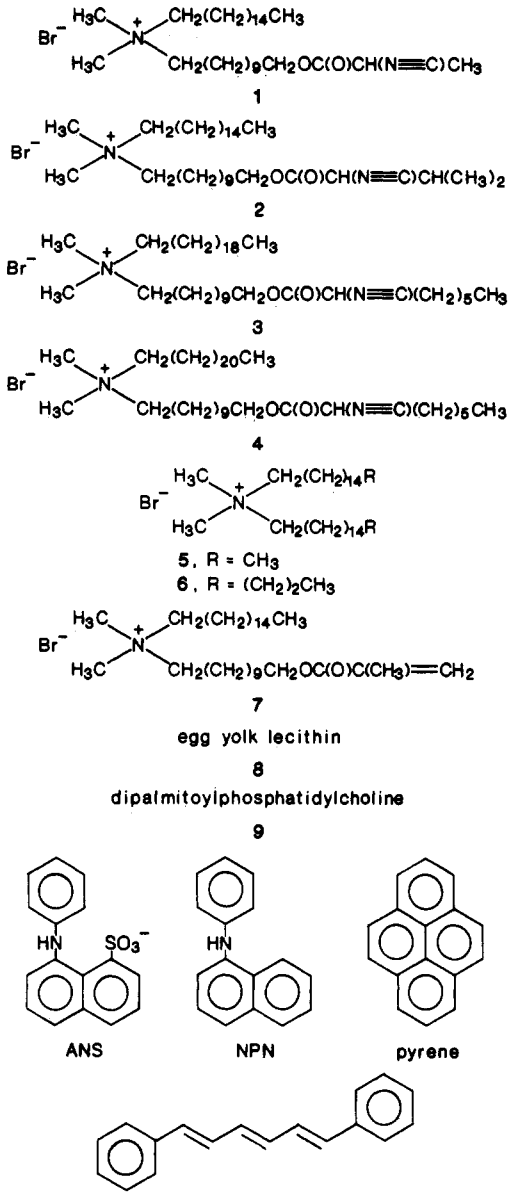

polymerized vesicles derived from the isocyano amphiphiles 1–4 (Chart I). In these amphiphiles the polymerizable isocyano group is located at different positions along the hydrocarbon chain. The fluorescence data are compared with data from electron microscopy, differential scanning calorimetry, and osmotic experiments. Measurements on vesicle systems prepared from dihexadecyldimethylammonium bromide (DHDAB) (5), dioctadecyldimethylammonium bromide (DODAB) (6), a polymerizable methacrylate amphiphile (7), first prepared by Regen,[6d] egg yolk lecithin (8), and dipalmitoylphosphatidylcholine (9) are also included. We report here on the changes in fluorescence that occur upon polymerization of the vesicle bilayers. These changes are discussed in terms of micropolarity and microviscosity.

Results

Synthesis of Isocyano Amphiphiles. Amphiphiles 1–4 were synthesized according to the general route outlined in Scheme I. 11-Bromoundecanol was reacted with the appropriate alkyldimethylamine to give the (11-hydroxyundecyl)ammonium bromides **10**. The latter bromides were coupled to *N*-formylated α-amino acids by

Scheme I

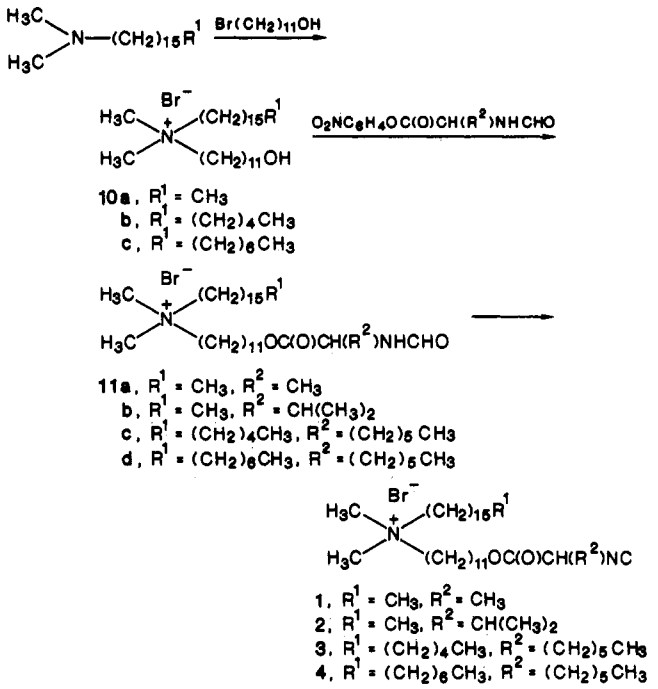

Table I
Phase Transition Temperatures of Polymerized and Unpolymerized Vesicles and Molecular Weight Data of Freeze-Dried Polymerized Vesicle Samples

compd[a]	T_c/°C	[η]/(dL/g)[b]	$\bar{M}_v$[c]	$\overline{DP}$
1u	−22 to −7			
1p	*d*	0.2	46000	75
2u	−26 to −16			
2p	*d*	0.1	31000	50
3u	−9 to −3			
3P	*d*	0.09	29000	40
4u	−20 to −13			
4p	*d*	<0.01	<8000	<11

[a] u = unpolymerized vesicles, p = polymerized vesicles. [b] In chloroform, 30.00 °C; estimated error ±0.03. [c] Calculated by using the Mark–Houwink equation $[\eta] = 1.4 \times 10^{-9} \times \bar{M}_w^{1.75}$; see ref 14b. [d] No phase transition observed.

means of the active ester method.[11] The resulting formamides were dehydrated[12] with phosphorus oxychloride and base to give isocyanides **1–4**. The amphiphiles showed characteristic isocyanide vibrations in the IR spectrum at approximately 2140 cm^{-1}. They were further characterized by ^1H NMR, MS, and elemental analysis.

Vesicle Formation. When amphiphiles 1–4 were dispersed in water, slightly opalescent solutions were obtained. Electron micrographs of these solutions, taken by the freeze-fracture technique, revealed the presence of spherical and ellipsoidal aggregates. The phase transition temperatures of these aggregates were determined by differential scanning calorimetry (DSC). The data are given in Table I. In order to establish the presence of closed structures, vesicle dispersions were prepared containing 0.1 M sucrose in their inner aqueous compartments. These dispersions were added to solutions of 0.01–0.4 M sucrose, and the absorbances at 450 nm (A_{450}) of the resulting mixtures were determined. The results are presented in Figure 1. For all isocyano amphiphiles, a linear relationship is found between $1/A_{450}$, which measures the vesicles' volume, and the reciprocal of the sucrose concentration. This indicates that the vesicle dispersions behave as almost ideal osmometers[13] and obey the van't Hoff law.

Table II
Fluorescence Data of ANS, NPN, Pyrene, and DPH Incorporated in Vesicles of 1-9[a]

	ANS			NPN		pyrene	DPH
compd[b]	λ_F[c,d]	sie[d,e]	r[f,g]	λ_F[c,h]	sie[e,h]	slope value[i]	r[f,j]
1u	488	1.7	0.05	433	1.2	14	0.06
1p	467	1.1	0.08	424	1.1	6	0.17
2u	479	1.6	0.06	428	1.2	24	0.07
2p	478	1.6	0.09	428	1.1	24	0.14
3u	476	1.4	0.10	422	1.2	21	0.08
3p	475	1.4	0.12	422	1.1	21	0.13
4u	476	1.3	0.10	422	1.2	16	0.10
4p	476	1.3	0.12	422	1.1	16	0.10
5	468	1.2	0.10	418	1.0	15	0.22
6	469	1.2	0.11	418	1.0	35	0.27
7u	479	1.4	0.06	422	1.2	18	0.09
7p	469	1.2	0.12	417	1.1	3	0.24
8	484	1.6		425	1.1		
9	478	1.4		424	1.1		

[a] Temperature 21 °C. [b] u = unpolymerized vesicles, p = polymerized vesicles. [c] Wavelength of maximum fluorescence intensity; estimated error 1 nm. [d] Excitation is at 375 nm. [e] Solvent isotope effect; estimated error 0.1. [f] Fluorescence anisotropy value; estimated error 0.01. [g] Excitation is at 375 nm; emission is measured at 473 nm. [h] Excitation is at 343 nm. [i] Slope of plot of I_E/I_M vs. mole fraction of pyrene; estimated error 0.5. [j] Excitation is at 355 nm; emission is measured at 430 nm.

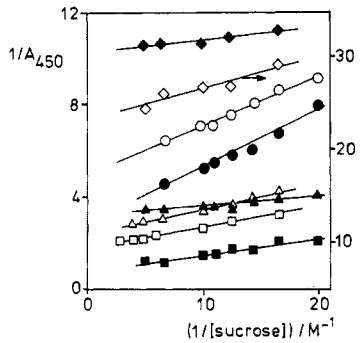

Figure 1. Relationship between the reciprocal of the absorbance at 450 nm of unpolymerized (u) and polymerized (p) vesicle dispersions and the reciprocal of the concentration of sucrose solutions in which the vesicles are osmotically treated until equilibrium: **1u** (◇); **1p** (◆); **2u** (△); **2p** (▲); **3u** (○); **3p** (●); **4u** (□); **4p** (■).

Vesicle Polymerization. Polymerization of the isocyano functions in the vesicle bilayers of 1–4 was achieved by adding nickel capronate.[6j,14]

$$n\mathrm{R{-}\overset{+}{N}{\equiv}\overset{-}{C}} \rightarrow [\mathrm{R{-}N{=}C{<}}]_n$$

In all cases polymerization was complete after 12 h. In the infrared spectrum of freeze-dried polymerized samples, the isocyanide stretching vibration at 2140 cm^{-1} had disappeared and a new band was visible at 1630 cm^{-1}, which we attribute to polymer N=C bonds. From the absence of a formyl stretching vibration at 1675 cm^{-1} we concluded that no significant hydrolysis of the isocyano functions in the vesicles had taken place. The polymerized vesicles were further characterized by electron microscopy (Figure 2), DSC (Table I, Figure 3), and sucrose experiments (Figure 1). In addition the intrinsic viscosities, $[\eta]$, of the freeze-dried polymerized samples were determined (Table I).

Fluorescence Measurements. ANS and NPN. The fluorescent probes 8-anilino-1-naphthalenesulfonate (ANS) and *N*-phenyl-1-naphthylamine (NPN) were added to already-formed polymerized and unpolymerized vesicles from amphiphiles 1–9. Subsequently, a fluorescence spectrum was recorded. In all measurements the molar ratio of amphiphile to probe was 250:1. The results are given in Table II. For comparison, fluorescence spectra of ANS and NPN were also measured in various dioxane–water mixtures. In Table III the fluorescence maxima are given together with the solvent polarities of the dioxane–water mixtures as expressed by the $E_T(30)$ parameter.[15]

Table III
Fluorescence Maxima of ANS and NPN Dissolved in Dioxane–Water Mixtures[a]

% dioxane (v/v) in water	E_T (30) value[b]	λ_F[c] ANS[d]	λ_F[c] NPN[e]
0	63.1	528	474
10	61.1	523	462
20	58.7	514	452
30	57.1	506	447
40	55.5	500	441
50	53.9	497	438
60	52.3	493	434
70	50.7	490	428
80	49.1	487	425
90	46.8	484	422
100	36.1	478	413

[a] Temperature 21 °C. [b] Values are taken from ref 15 or derived from values therein by linear interpolation. [c] Wavelength of maximum fluorescence intensity. [d] Excitation is at 375 nm. [e] Excitation is at 343 nm.

The fluorescence spectra of ANS and NPN change when D_2O is substituted for water.[7a,f,16] The fluorescence intensities increase whereas the positions of the fluorescence maxima remain unaffected. The ratio of the intensity in D_2O and in water is called the solvent isotope effect (sie). It is a relative measure for the amount of water present in the probe's microenvironment. On exposing ANS and NPN to 100% water, we measured sie values of 2.5 and 2.0, respectively, which is in agreement with literature data.[7a,f,16] The values obtained when the probes are incorporated in the various polymerized and unpolymerized vesicle systems are presented in Table II.

Pyrene. The fluorescence spectrum of pyrene shows, at low concentrations, a so-called monomer band with a vibrational fine structure in the wavelength range 370–420 nm. When the concentration is increased, a second band, without fine structure, called the excimer band, appears at 475 nm. The intensity ratio of the excimer band to the monomer band, I_E/I_M, can be correlated to the fluidity of the system.[17] For pyrene incorporated in vesicles of 1–7 this ratio was measured at probe concentrations of (0.1–1.0) $\times 10^{-4}$ M and at an amphiphile concentration of 5×10^{-3} M. The results of these experiments are given in Figure 4 and in Table II.

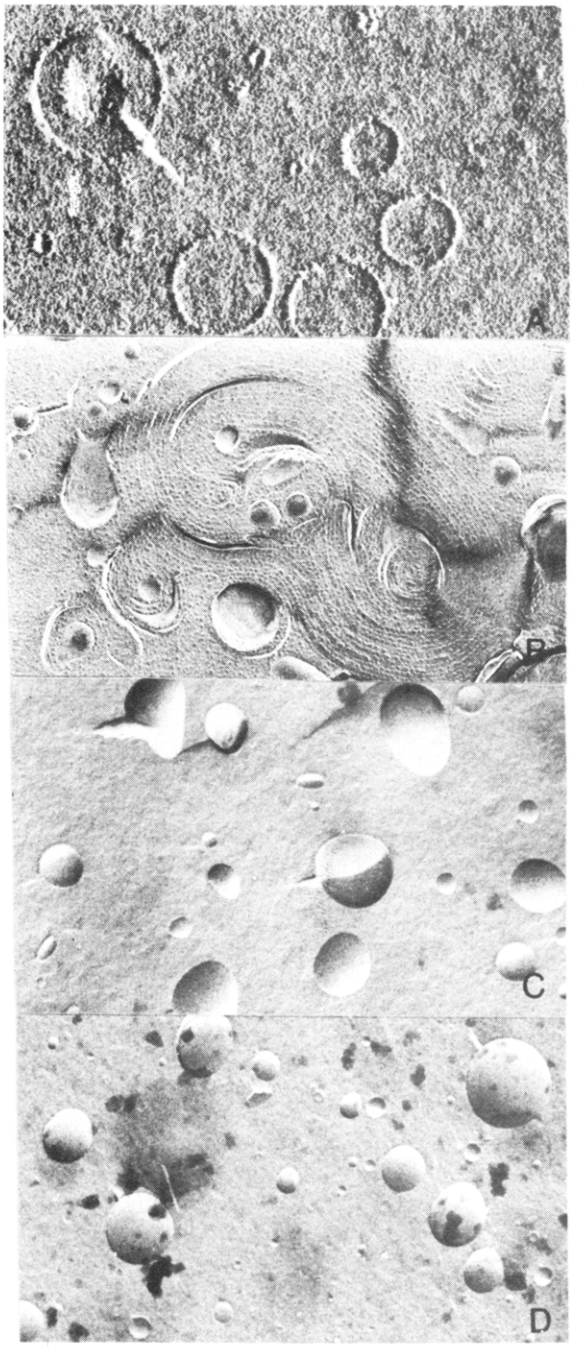

Figure 2. Freeze-fracture electron micrographs of polymerized vesicles derived from **1** (A, magnification ×100 000), **2** (B, ×20 000), **3** (C, ×40 000), and **4** (D, ×40 000).

DPH. Fluorescence depolarization experiments[18] were carried out on vesicles of **1–7** labeled with the probe 1,6-diphenyl-1,3,5-hexatriene (DPH). In Table II the anisotropy values of DPH fluorescence are given. Results of similar experiments on vesicles labeled with ANS are also presented in this table.

Discussion

Structure of the Bilayers. Polymers of isocyanides have a rigid, helical configuration with four repeating units per helical turn.[14] The polymer side chains point away from the central axis as shown in Figure 5C. On polymerization, the surfactant chains of amphiphiles **1–4** will cross-link in a direction parallel to the vesicle surface. Polymer links may be formed either in one-half of the bilayer (Figure 5B) or between the bilayer halves (Figure 5A). A schematic representation of the networks formed

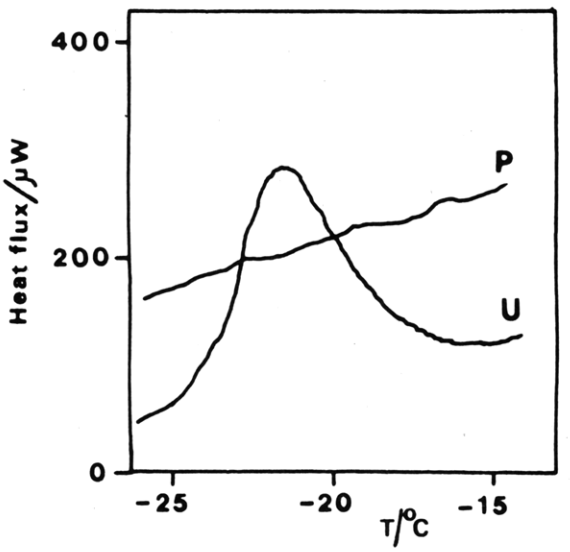

Figure 3. Differential scanning calorimetry heating curves of unpolymerized (u) and polymerized (p) vesicles of **2**.

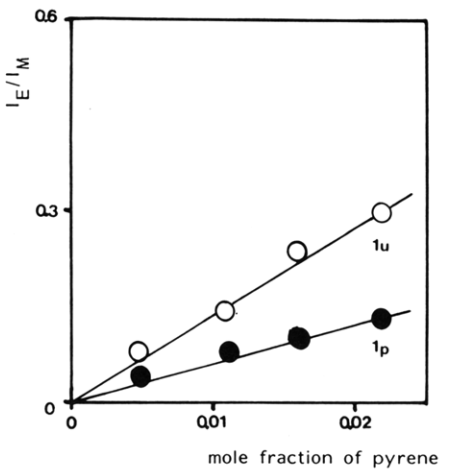

Figure 4. Plot of I_E/I_M vs. the mole fraction of pyrene in unpolymerized (u) and polymerized (p) vesicles of **1**.

in this way is given in Figure 5D. The average length of the polymer chains can be roughly estimated from the molecular weight data in Table I.[19] For amphiphiles **1–4** these lengths amount to 76, 49, 40, and <11 Å, respectively. Apparently, polymerization proceeds less facilely going from **1** to **4**. Increasing steric hindrance from the bulky side groups is probably the reason for this behavior.

In a previous paper[6j] we reported that freeze-fracture electron microscopy may give information on the polymerization process in the vesicles, in particular whether linking of the surfactant chains occurs across the bilayer or within each of the monolayers. We discussed the differences in electron microscopic patterns of polymerized and unpolymerized vesicles of **1**. The unpolymerized aggregates appear as concave and convex half-spheres and half-ellipsoids, whereas the polymerized vesicles are visible as circles and ellipses (Figure 2A). We explained this phenomenon by a different fracturing behavior of the two types of vesicles. In the unpolymerized system the fracture plane runs through the middle of the bilayer (Figure 6A).[20] In the polymerized one, the particles are cross-fractured (Figure 6B). The reason for this is that in compound **1** the polymerizable group is at the end of the surfactant chain, making cross-linkage of the monolayers as well as the bilayer possible. The special 4^1-helical structure of the polymeric backbone with its side chains pointing toward

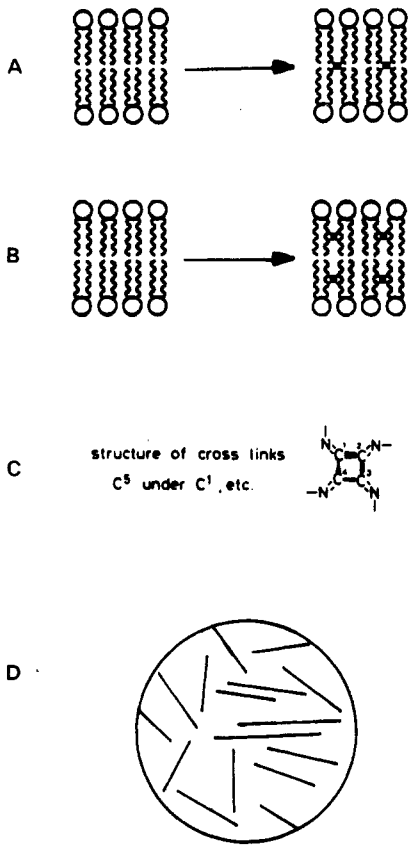

Figure 5. Trans-bilayer (A) and monolayer (B) cross-linking in vesicles of isocyano amphiphiles. Structure of cross-links that are formed during polymerization of isocyanide functions (C). Schematic representation of the networks obtained after polymerization (D); the polymeric rods are oriented parallel to the vesicle surface.

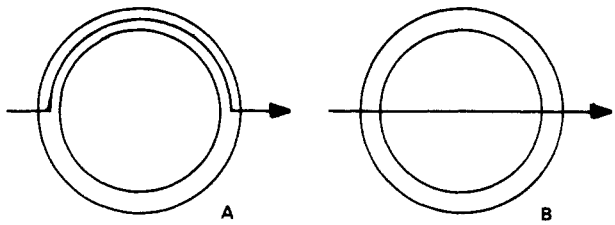

Figure 6. Fracturing behavior of unpolymerized and polymerized vesicles during the freeze-fracturing process. The fracture plane runs through the middle of the bilayer (A) or traverses the vesicle (B).

both monolayers facilitates this cross-linking process. This efficient cross-linking prevents the bilayer from splitting.

Electron micrographs of unpolymerized vesicle dispersions of **2**–**4** (not shown) and also of polymerized vesicles of **3** and **4** (Figure 2C,D) displayed patterns similar to that of unpolymerized **1**. Polymerized vesicles of **2** are portrayed as half-spheres and as ellipse-like structures (Figure 2B). We explain these features in the following way. On going from **1** to **4** the distance between the polymerizable group and the end of the fatty chain increases. As a result, cross-linking of the bilayer halves will gradually become more difficult and polymerization will occur preferentially within each of the monolayers. The position of the isocyano group in amphiphile **2** apparently still allows some transbilayer cross-linking and thus cross-fracturing of the vesicles to occur, especially in large vesicles. On going from **1**–**4** the degree of polymerization of the surfactant chains becomes lower (Table I). This could also explain why cross-fracturing is less likely to occur in compounds **2**–**4** than in compound **1**.

The osmotic experiments (Figure 1) indicate that the vesicles formed from amphiphiles **1**–**4** are closed aggregates. They are able to entrap molecules and do not leak. Polymerization does not affect this behavior.

DSC measurements show that the unpolymerized vesicles of **1**–**4** have phase transitions at temperatures below 0 °C (Table I).[22] Therefore, at room temperature, the vesicle bilayers are in the fluid state. Compared to DODAB (T_c = 51 °C[23]) and DHDAB (T_c = 44 °C[23]) the phase transition temperatures of **1**–**4** have lowered considerably. This lowering may be caused by the bulkiness of the fatty chains and the relatively high polarity of the polymerizable end-group functions. These factors both tend to perturb the ordening of the hydrocarbon chains.[24] The polymerized vesicles do not show phase transitions anymore. A similar observation was made by Wagner et al.[25] on polymerized vesicles of a diacetylene amphiphile.

Polarity of the Bilayers. ANS and NPN are probes both of polarity and viscosity. It has been suggested that the emission wavelength of the probe is a measure of the polarity of the medium, if the solvent relaxation of the excited state is completed within the fluorescence lifetime.[7c,8,26] Whether this is the case of our unpolymerized vesicle systems was tested by exciting 20 nm above the excitation maximum. We found that for all systems the emission maxima of ANS and NPN remained at the same place, suggesting that solvent relaxation is always complete.[27] Evidence exists in the literature[28] that the negatively charged probe ANS binds just below the vesicle surface with its sulfonic acid group directed toward the aqueous phase. Unlike ANS, the neutral probe NPN is only sparingly soluble in water. Therefore, this compound is assumed to be located in the hydrophobic core of the membrane.[28] The fluorescence measurements in the series of dioxane–water mixtures (Table III) show that the emission maxima of ANS and NPN shift to longer wavelengths with increasing polarity of the medium. In Figure 7 the fluorescence wavelengths of ANS and NPN in the various vesicle systems are compared. From the location of the emission maxima it appears that both ANS and NPN are located in a relatively apolar (more dioxane-like) environment.[29] There are, however, differences between the various systems. When ANS and NPN are bound to DHDAB or DODAB vesicles, their fluorescence maxima are at somewhat shorter wavelengths than when they are bound to unpolymerized vesicles of **1**–**4** and **7**. Apparently, the bilayers of the former vesicles have a lower polarity than those of the latter ones. One reason may be the presence of the polar functions (isocyanide and ester functions) in **1**–**4** and **7**. Another reason could be that at the temperature of the measurements, **5** and **6** are in the solid state, whereas **1**–**4** and **7** are in the fluid state. The latter state could allow for a higher degree of water penetration (vide infra).

The extent of water penetration in the vesicle bilayers can be deduced from the fluorescence experiments in D_2O and in water. As mentioned in the Results, the fluorescence intensity of ANS and NPN is higher in D_2O than in water by a factor of 2.5 and 2.0, respectively. This difference in intensity is due to the fact that water quenches the fluorescence of the probe more effectively than D_2O does. The mechanism of this quenching is not fully understood yet.[30] In Figure 8 the solvent isotope effects, $I(D_2O)/I(H_2O)$, for ANS and NPN in the various polymerized and unpolymerized vesicle systems are plotted vs. the corresponding fluorescence wavelengths. For ANS a straight line is obtained with a slope significantly different from zero. This suggests that the observed polarity

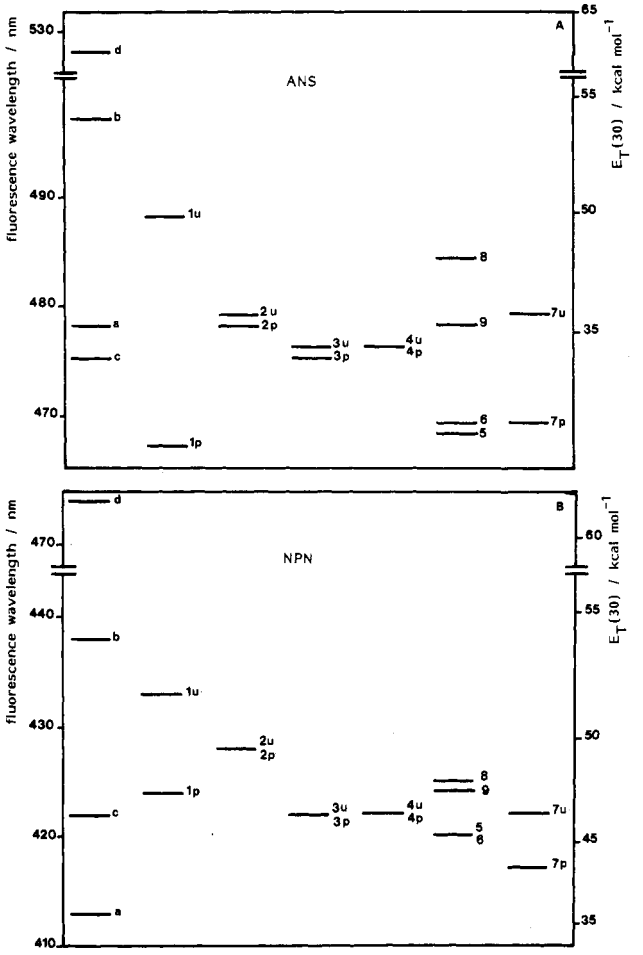

Figure 7. Fluorescence data of ANS (A) and NPN (B) in various solvents and vesicle systems. a = dioxane, b = 1:1 (v/v) dioxane–water, c = ethanol, and d = water. For numbering of compounds see Chart I; u = unpolymerized vesicles and p = polymerized vesicles.

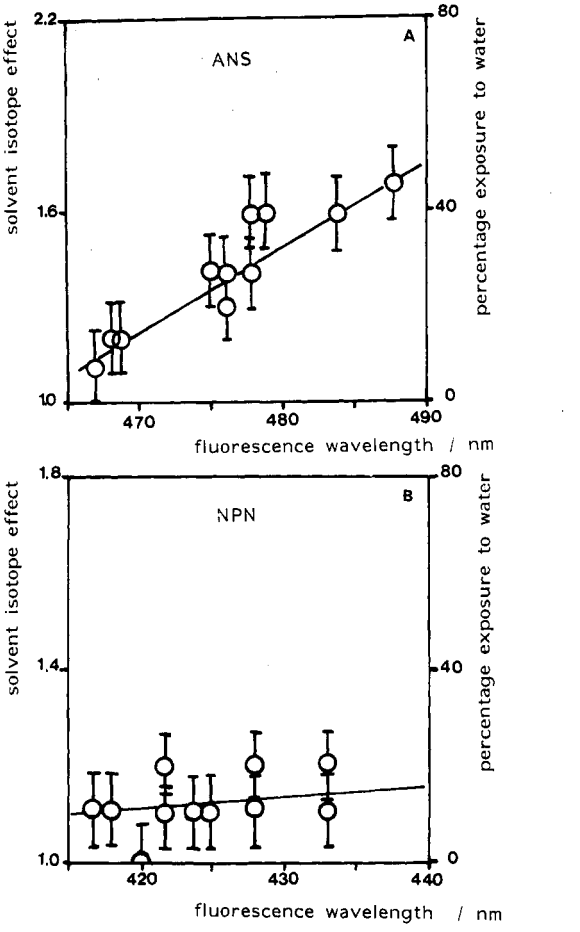

Figure 8. Plots of solvent isotope effect vs. fluorescence wavelength for ANS (A) and NPN (B) in the various vesicle systems; data are taken from Tables II and IV.

differences near the surface of the bilayer are mainly due to differences in water penetration. For NPN the solvent isotope effect does not vary with the fluorescence wavelength. Apparently, water penetration in the inner parts of the vesicle bilayers is relatively low. We may conclude that the observed polarity differences in this region mainly result from differences in structure of the hydrophobic tails, in particular the presence or absence of polar groups.

Polymerization of vesicles of **1** causes the fluorescence maximum of ANS to shift to shorter wavelengths (Figure 7). We ascribe this phenomenon to a lower degree of water penetration in the bilayer due to a closer packing of the fatty chains in the polymerized aggregates. The solvent isotope effect (Table II) supports this hypothesis. For NPN the blue shift observed after polymerization is probably not related to a change in water penetration, but is more likely to be caused by the disappearance of the isocyano functions. For ANS and NPN incorporated in polymerized and unpolymerized vesicles of **7** a fluorescence behavior is observed similar to that of **1**. The observed shifts and differences in solvent isotope effect, however, are smaller, reflecting the difference in chemical structure of the two types of polymerized and unpolymerized vesicles.

The fluorescence maximum of ANS in vesicles of **2–4** does not change on polymerization of the aggregates. We can partly explain this phenomenon by the lower degree of polymerization of the isocyano functions in these vesicles. Another reason could be that since the cross-links are in the middle part of the chains instead of at the end, the amphiphilic molecules are less closely packed. This could allow for a substantial penetration of water. On polymerization of **2–4** the fluorescence maximum of NPN does not change either. Apparently, this probe is not located in the vicinity of the polymerizable functions, as it was in vesicles of **1**.

Figure 7 shows that the fluorescence maxima of ANS in egg yolk lecithin (**8**) and in DPPC (**9**) lie at different wavelength positions. In these vesicle systems, approximately the same values are obtained for the maxima of NPN. At the measurement temperature (25 °C) egg yolk lecithin is in the fluid state, whereas DPPC is in the solid state. This difference in state has no influence on NPN fluorescence, but does have one on ANS, as it allows for a higher degree of water penetration in the surface region.

Viscosity of the Bilayers. Fluorescence depolarization is a useful technique for evaluating the fluidity of bilayer membranes.[18] DPH is often used as a probe in these experiments. This compound is believed to be located in the inner part of the bilayer matrix.[18] In Figure 9 the fluorescence anisotropy data of Table II are represented graphically. The anisotropy values of DPH fluorescence are considerably higher in DHDAB (**5**) and DODAB (**6**) than in the other unpolymerized vesicle systems. The reason for this is that at the measurement temperature both DHDAB and DODAB are in the solid state, which limits molecular motion. Unpolymerized vesicles of **1–4** are all in the fluid state. This results in lower anisotropy values (Figure 9). On polymerization of vesicles of **1**, the anisotropy of DPH fluorescence increases significantly, indicating that molecular motion is restricted in the polymerized state. Figure 9A shows that for **1–4** the dif-

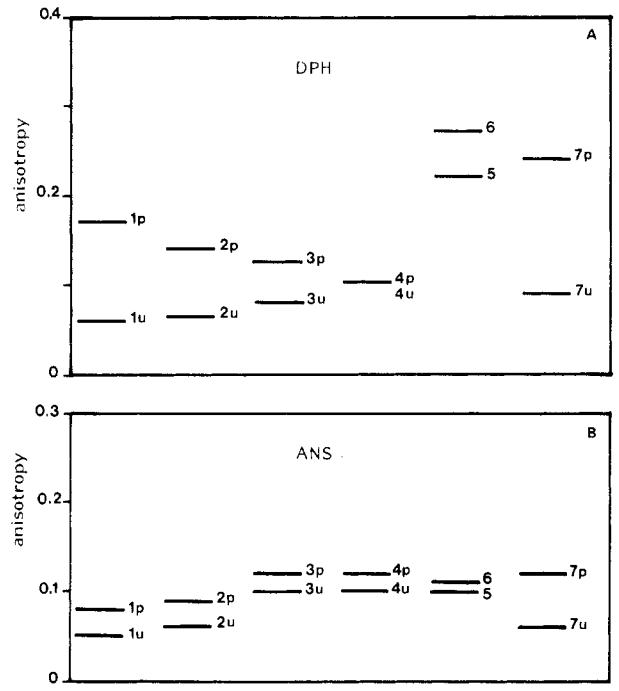

Figure 9. Fluorescence anisotropy values of DPH (A) and ANS (B) in polymerized and unpolymerized vesicles. For numbering of compounds see Chart I; u = unpolymerized vesicles and p = polymerized vesicles.

ference in anisotropy between the polymerized and unpolymerized vesicles gradually becomes smaller. This trend can be correlated to the trend in polymerized **1**–**4** of decreasing molecular weight. For compounds **1**–**6** the fluorescence anisotropy values of ANS are all in the same range and vary only slightly on going from the unpolymerized to the polymerized state (Figure 9B). One reason for this slight variation is that in depolarization experiments ANS is a less sensitive probe than DPH. Another reason could be that the molecular motion of the surfactant chains in the head-group region is not influenced by the structure of the amphiphiles. Compound **7** seems to be in discord with the other compounds, as it shows a larger change in anisotropy on going from the unpolymerized to the polymerized state.

Pyrene is another probe frequently used to measure membrane fluidity.[17] It shows two emission maxima, one originating from single excited pyrene molecules (P*) and a second one originating from complexes between an excited molecule P* and a ground-state molecule P, so-called excimers (PP*). The extent of excimer formation is dependent on the degree of lateral diffusion in the membrane.[17] When the intensity ratio of the excimer peak and the monomer peak, I_E/I_M, is measured as a function of pyrene concentration, a straight line is obtained. The slope of this line is related to the viscosity of the system. This viscosity can be calculated provided that the concentration of the probe in the bilayer is known. For our vesicle systems, this concentration is difficult to calculate, as the volume of the bilayer cannot be determined accurately.

In Figure 4 the I_E/I_M values for unpolymerized and polymerized vesicles of **1** are plotted vs. the mole fraction of pyrene, X_{pyr} = (moles of pyrene)/(moles of pyrene + moles of amphiphile). It is evident from this figure that polymerization of the bilayers of **1** leads to less excimer formation. This can be ascribed to a decrease in membrane viscosity on polymerization. No significant changes occur when vesicles of **2**–**4** are polymerized (Table II). Apparently, the changes in viscosity are too low to be detected by pyrene. Vesicles of amphiphile **7** behave similarly to those of amphiphile **1**. On polymerizing, also a decrease in excimer formation is observed.

The slope of the I_E/I_M vs. mole fraction plot is considerably higher for DODAB (**6**) than for the other amphiphiles. As the bilayers of DODAB are more densely packed at the measurement temperature, this could promote the formation of clusters of pyrene molecules.[17c] This explanation is supported by the fact that DODAB shows an abrupt decrease in the I_E/I_M ratio at the phase transition temperature.[31,32] A similar decrease was observed for DPPC vesicles.[17c,33]

Experimental Section

Infrared, UV–vis, and fluorescence spectra were recorded on Perkin-Elmer 283, 555, and 650-40 spectrometers, respectively. Fluorescence depolarization experiments were carried out on an apparatus built by the group of Prof. Y. K. Levine.[34] ^{1}H NMR spectra were obtained on Varian EM 390 and Bruker WP 200 instruments. Chemical shifts are given downfield from internal tetramethylsilane. Abbreviations used are s = singlet, d = doublet, t = triplet, m = multiplet, and b = broad. Electron microscopy was carried out with a Philips EM 301 instrument. Samples were frozen in a slush of liquid and solid nitrogen, fractured with a Denton freeze etch apparatus, and replicated with Pd/C according to standard procedures.[35] Glycerol was added up to 25% to prevent feeze damage. Mass spectra were recorded on an AEI MS-902 mass spectrometer. Elemental analyses were done by the Elemental Analytical Section of the Institute for Applied Chemistry TNO, Utrecht. Differential scanning calorimetry measurements were carried out on a Setaram DSC 111 instrument. Solution viscosity data were obtained on freeze-dried polymerized vesicle samples, using a Cannon-Ubbelohde viscometer in chloroform at 30.00 °C. Viscosity-average molecular weights were calculated by using the Mark–Houwink equation $[\eta] = 1.4 \times 10^{-9}\bar{M}_w^{1.75}$.[14b] Since aggregation of the polymer chains can occur as a result of charge clustering, the calculated molecular weights (Table I) must be regarded as an estimation.[39]

Unless otherwise stated all chemicals and reagents were commercial products and were used without further purification. Water used for the preparation of the vesicles was doubly distilled in an all-quartz apparatus. 8-Anilino-1-naphthalenesulfonic acid ammonium salt and *N*-phenyl-1-naphthylamine were purchased from Sigma and Aldrich, respectively. Pyrene was obtained from Janssen and 1,6-diphenyl-1,3,5-hexatriene was a gift from Prof. Y. K. Levine. 11-Bromoundecanol was prepared from 11-bromoundecanoic acid (Aldrich) according to literature procedures.[36] Dimethylhexadecylamine, dimethyleicosylamine, and dimethyldocosylamine were prepared from hexadecyl bromide, eicosyl bromide, and docosyl bromide, respectively, by reaction with dimethylamine.[37] Dimethylhexadecyl[11-[[(2-propenyl)-carbonyl]oxy]undecyl]ammonium bromide (**7**) was prepared according to the procedure given by Regen et al.[6d]

Dihexadecyldimethylammonium Bromide (5). This compound was prepared by refluxing hexadecyldimethylamine and hexadecyl bromide in toluene for 16 h. After removal of the solvent the crude solid was washed thoroughly with ether and recrystallized from acetone: yield 89% of a white solid; ^{1}H NMR ($CDCl_3$) δ 0.85 (t, 6 H, CH_3), 1.05–1.85 (m, 56 H, CH_2), 3.35–3.70 (m, 10 H, CH_3N, CH_2N).

Dioctadecyldimethylammonium Bromide (6). This compound was prepared from octadecyldimethylamine and octadecyl bromide as described for **5**: yield 86% of a white solid; ^{1}H NMR ($CDCl_3$) δ 0.85 (t, 6 H, CH_3), 1.05–1.85 (m, 60 H, CH_2), 3.35–3.70 (m, 10 H, CH_3N, CH_2N).

The *p*-nitrophenyl esters of *N*-formylalanine, *N*-formylvaline, and (*N*-formylamino)caproic acid were prepared by reacting these compounds with *p*-nitrophenol and dicyclohexylcarbodiimide in pyridine.[38]

***N*-Formylalanine 4-Nitrophenyl Ester**: yield 81% of a white solid; ^{1}H NMR ($CDCl_3$) δ 1.6 (d, 3 H, CH_3), 4.95 (m, 1 H, CH), 6.20 (b, 1 H, NH), 7.27 (d, 2 H, ArH), 8.30 (m, 3 H, ArH, CHO).

***N*-Formylvaline 4-Nitrophenyl Ester**: yield 70% of a white solid; ^{1}H NMR ($CDCl_3$) δ 1.0–1.1 (d, 6 H, CH_3), 2.4 (m, 1 H, CH), 4.9 (m, 1 H CHN), 6.8 (b, d, 1 H, NH), 7.3 (d, 2 H, ArH), 8.3 (m, 3 H, ArH, CHO).

2-(*N*-Formylamino)caproic Acid 4-Nitrophenyl Ester: yield 77% of a white solid; ^{1}H NMR ($CDCl_3$) δ 0.9 (t, 3 H, CH_3), 1.0–2.2 (m, 10 H, CH_2), 4.9 (m, 1 H, CH), 6.6 (b, 1 H, NH), 7.3 (d, 2 H, ArH), 8.3 (m, 3 H, ArH, CHO).

Dimethylhexadecyl(11-hydroxyundecyl)ammonium Bromide (10a). Dimethylhexadecylamine (5.57 g, 0.021 mol) and 11-bromoundecanol (5.20 g, 0.021 mol) were dissolved in toluene (50 mL) and refluxed for 18 h. The solvent was evaporated and the resulting solid washed with ether: yield 9.4 g (87%) of almost pure product; ^{1}H NMR ($CDCl_3$) δ 0.85 (t, 3 H, CH_3), 1.05–1.85 (m, 46 H, CH_2), 3.35–3.70 (m, 12 H, CH_3N, CH_2N, CH_2O). Anal. Calcd for $C_{29}H_{62}BrNO\cdot{}^1/_2H_2O$: C, 65.75; H, 11.99; N, 2.64. Found: C, 65.89; H, 11.92; N, 2.69.

Dimethylhexadecyl[11-[[[1-(*N*-formylamino)ethyl]carbonyl]oxy]undecyl]ammonium Bromide (11a). Compound **10a** (8 g, 0.015 mol) and dry triethylamine (1.55 g, 0.015 mol) were dissolved in chloroform (50 mL) and added dropwise at 0 °C to a solution of *N*-formyl-L-alanine *p*-nitrophenyl ester (7.32 g, 0.031 mol) in chloroform (50 mL). The mixture was stirred at room temperature for 72 h. The solvent was evaporated and the resulting solid purified by column chromatography (silica gel, eluent 9:1 (v/v) chloroform–methanol): yield 5.5 g (60%) of oil; IR (neat) 1740 (CO) 1675 (NHCO) cm^{-1}; ^{1}H NMR ($CDCl_3$) δ 0.85 (t, 3 H, CH_3), 1.15–1.85 (m, 49 H, CH_2 and CH_3), 3.33–3.65 (m, 10 H, CH_3N and CH_2N), 4.13 (t, 2 H, CH_2O), 4.63 (m, 1 H, CHN), 6.67–6.87 (b, d, 1 H, NH), 8.2 (s, 1 H, CHO). Anal. Calcd for $C_{33}H_{67}BrN_2O_3\cdot H_2O$: C, 62.14; H, 10.90; N, 4.39. Found: C, 62.46; H, 10.99; N, 3.82.

Dimethylhexadecyl[11-[[(1-isocyanoethyl)carbonyl]oxy]undecyl]ammonium Bromide (1). To a solution of the preceding formamide (0.8 g, 1.3 mmol) and triethylamine (0.76 g, 7.5 mmol) in methylene chloride (25 mL) was added dropwise at 0 °C phosphorus oxychloride (0.59 g, 3.8 mmol) in methylene chloride (10 mL). The mixture was stirred at room temperature for 20 h. Hereafter, it was added slowly, while stirring, to aqueous Na_2CO_3 (40 mL, 7.5% solution). The organic layer was separated, dried (Na_2SO_4), and concentrated under vacuum. The product was purified by column chromatography (silica gel, eluent 9:1 (v/v) chloroform–methanol): yield 0.5 g (64%) of almost pure isocyanide; IR (neat) 2145 (NC), 1750 (CO) cm^{-1}; ^{1}H NMR ($CDCl_3$) δ 0.87 (t, 3 H, CH_3), 1.10–1.80 (m, 49 H, CH_2), 3.30–3.63 (m, 10 H, CH_3N and CH_2N), 4.17 (t, 2 H, CH_2O), 4.30 (m, 1 H, CH). Anal. Calcd for $C_{33}H_{65}BrN_2O_2\cdot{}^1/_2H_2O$: C, 63.03; H, 10.90; N, 4.45. Found: C, 63.36; H, 11.00; N, 4.24.

Dimethylhexadecyl[11-[[[1-(*N*-formylamino)-2-methylpropyl]carbonyl]oxy]undecyl]ammonium Bromide (11b). Procedures used were similar to those described above for the preparation of **11a**: yield 57% of a colorless oil; IR (neat) 1740 (CO), 1675 (NHCO) cm^{-1}; NMR ($CDCl_3$) δ 0.8–1.1 (m, 9 H, CH_3), 1.1–1.9 (m, 46 H, CH_2), 2.2 (m, 1 H, CH), 3.3–3.7 (m, 10 H, CH_3N, CH_2N), 4.2 (t, 2 H, CH_2O), 4.6 (m, 1 H, CH), 6.5 (br, 1 H, NH), 8.3 (s, 1 H, CHO).

Dimethylhexadecyl[11-[[(1-isocyano-2-methylpropyl)carbonyl]oxy]undecyl]ammonium Bromide (2). Procedures used were similar to those described above for the preparation of 1: yield 58% of a colorless waxlike substance; IR (neat) 2145 (NC), 1745 (CO) cm^{-1}; ^{1}H NMR ($CDCl_3$) δ 1.1 (m, 9 H, CH_3), 1.2–2.0 (m, 46 H, CH_2), 2.4 (m, 1 H, CH), 3.4–3.8 (m, 10 H, CH_3N, CH_2N), 4.3 (m, 3 H, CH_2O, CH); MS *m/e* 534 ($M^+ - CH_3Br$). Anal. Calcd for $C_{35}H_{69}BrN_2O_2\cdot 1{}^1/_4H_2O$: C, 64.47; H, 10.97; N, 4.30; O, 7.98. Found: C, 64.07; H, 11.41; N, 4.27; O, 7.97.

Dimethyleicosyl(11-hydroxyundecyl)ammonium Bromide (10b). Procedures used were similar to those described above for the preparation of **10a**: yield 52% of a white solid; ^{1}H NMR ($CDCl_3$) δ 0.9 (t, 3 H, CH_3), 1.0–1.6 (m, 54 H, CH_2), 3.1–3.4 (m, 12 H, CH_2N, CH_3N, CH_2O).

Dimethyleicosyl[11-[[[1-(*N*-formylamino)heptyl]carbonyl]oxy]undecyl]ammonium Bromide (11c). Procedures used were similar to those described above for the preparation of **11a**: yield 72% of a colorless waxlike substance; IR (neat) 1740 (CO), 1675 (CO) cm^{-1}; ^{1}H NMR ($CDCl_3$) δ 0.9 (t, 6 H, CH_3), 1.0–2.0 (m, 62 H, CH_2), 3.3–3.7 (m, 10 H, CH_3N, CH_2N), 4.2 (t, 2 H, CH_2O), 4.7 (m, 1 H, CH), 6.5 (d, br, 1 H, NH), 8.1 (s, 1 H, CHO).

Dimethyleicosyl[11-[[(1-isocyanoheptyl)carbonyl]oxy]undecyl]ammonium Bromide (3). Procedures used were similar to those described above for the preparation of 1: yield 61.9% of a colorless oil; IR (neat) 2143 (NC), 1750 (CO) cm^{-1}; ^{1}H NMR ($CDCl_3$) δ 0.9 (t, 6 H, CH_3), 1.0–2.0 (m, 64 H, CH_2), 3.0–3.6 (m, 10 H, CH_3N, CH_2N), 4.2 (m, 3 H, CH, CH_2O); MS *m/e* 631 ($M^+ - CH_3Br$). Anal. Calcd for $C_{42}H_{83}BrN_2O_2\cdot{}^3/_4H_2O$: C, 68.06; H, 11.41; N, 3.78; O, 5.94. Found: C, 68.12; H, 11.69; N, 3.56; O, 5.82.

Dimethyldocosyl(11-hydroxyundecyl)ammonium Bromide (10c). Procedures used were similar to those described for the preparation of **10a**: yield 72% of a white solid; ^{1}H NMR ($CDCl_3$) δ 0.9 (t, 3 H, CH_3), 1.0–1.6 (m, 58 H, CH_2), 3.0–3.6 (m, 12 H, CH_3N, CH_2N, CH_2O).

Dimethyldocosyl[11-[[[1-(*N*-formylamino)heptyl]carbonyl]oxy]undecyl]ammonium Bromide (11d). Procedures used were similar to those described above for the preparation of **11a**: yield 61% of a colorless waxlike substance; IR (neat) 1740 (CO), 1675 (CO) cm^{-1}; ^{1}H NMR ($CDCl_3$) δ 0.9 (t, 6 H, CH_3), 1.0–2.0 (m, 66 H, CH_2), 3.4–3.7 (m, 10 H, CH_3N, CH_2N), 4.1–4.3 (t, 2 H, CH_2O), 4.5–4.8 (m, 1 H, CH), 6.5 (br, 1 H, NH), 8.3 (s, 1 H, CHO).

Dimethyldocosyl[11-[[(1-isocyanoheptyl)carbonyl]oxy]undecyl]ammonium Bromide (4). Procedures used were similar to those described above for the preparation of 1: yield 45.3% of a white solid; IR (neat) 2143 (NC), 1750 (CO) cm^{-1}; ^{1}H NMR ($CDCl_3$) δ 0.9 (t, 6 H, CH_3), 1.0–2.0 (m, 68 H, CH_2), 3.4–3.8 (m, 10 H, CH_3N, CH_2N), 4.1–4.3 (m, 3 H, CH, CH_2O); MS *m/e* 634 ($M^+ - CH_3Br$). Anal. Calcd for $C_{44}H_{87}BrN_2O_2\cdot H_2O$: C, 68.37; H, 11.60; N, 3.62; O, 6.21. Found: C, 68.03; H, 11.91; N, 3.39; O. 6.47.

Preparation of Vesicles. Vesicles were prepared by the following procedures. Initial surfactant concentrations amounted to 5×10^{-2} M. Amphiphiles 1–4 were dispersed in water by vortexing for 1 min. The slightly opalescent dispersions were used as such. Amphiphile **7** was dispersed first by vortexing for 1 min and subsequently by sonicating in a bath-type sonicator (Sonicor SC-52) for 30 min at 60 °C. DHDAB (**5**) and DODAB (**6**) were dispersed by sonicating for 6 min at 75 °C using a microtip of a Branson Sonifer B-12 set at 40 W. Subsequently, the vesicles were centrifuged at 5000 rpm for 15 min to remove titanium particles from the tip. Egg yolk lecithin (**8**) and DPPC (**9**) were obtained from Prof. J. de Gier as stock solutions (0.1 M) in chloroform–methanol (4:1 (v/v)). The solvent was evaporated under vacuum for about 1.5 h. Hereafter, water and a glass bead were added and the residue was swirled gently at 37 °C. The milky liposome dispersions thus obtained were sonicated in a bath-type sonicator at 37 °C for 30 min.

Vesicle Polymerization. A solution of nickel capronate in methanol (0.01 mL, 0.09 M) was brought into a test tube. The methanol was removed under a stream of nitrogen and a vesicle dispersion of 1–4 in water (0.5 mL, 5×10^{-2} M) was added. The mixture was vortexed for 1 min at 25 °C and kept at this temperature for 12 h. Polymerization of dispersions of **7** was carried out by direct UV irradiation (254 nm, Philips HPLN 125W E73-2 without bulb) for 3 h.

Osmotic Experiments. A stock solution was prepared by vortexing 1–4 (0.06 mmol) in 0.6 mL of water containing 0.1 M sucrose. Small aliquots (0.005 mL) of this stock solution were added to 0.25 mL of solutions containing 0.01–0.04 M sucrose. Three minutes after mixing, the turbidity was measured at 450 nm. A stock solution of polymerized vesicles was prepared as follows. Compounds 1–4 were dispersed in 0.1 M sucrose as described above. Subsequently, 2.1×10^{-3} mmol of nickel capronate was added and the mixture was kept at 30 °C for 12 h. With this stock solution, the same experiments were performed as described above.

Sample Preparation Fluorescence Experiments. ANS and NPN. For the experiments, freshly prepared stock solutions of ANS and NPN (10^{-2} M) in methanol were used, which were kept in the dark. To a unpolymerized or polymerized vesicle dispersion (0.1 mL, 5×10^{-2} M) the probe solution (0.002 mL) was added and the mixture was vortexed at 20 °C for 30 s. The presence of the methanol did not influence the measurements, as was checked separately. The vesicle dispersions thus obtained were allowed to stand for 0.5 h in order to get full penetration of the probe molecules into the vesicle bilayers. For the fluorescence measurements samples of the vesicle dispersions (0.02 mL), were diluted with water or D_2O (1.0 mL) by vortexing for 30 s. Final amphiphile and probe concentrations amounted to 10^{-3} and 4×10^{-6} M, respectively.

Pyrene. In all experiments with this probe, oxygen was carefully excluded. Freshly distilled water was boiled for 1 h under a nitrogen atmosphere just before use. Stock solutions of pyrene (0.02 mL, (0.2–1) × 10^{-2} M) were prepared in degassed methanol and brought into test tubes where the methanol was evaporated under a stream of nitrogen. To each tube a vesicle dispersion (0.2 mL, 5 × 10^{-2} M) and water (1.8 mL) were added. The samples were vortexed, degassed for 15 min, and shaken for 30 min with a Griffin flask shaker in order to get full solubilization of the pyrene. Final amphiphile and pyrene concentrations amounted to 5 × 10^{-3} and (0.2–1) × 10^{-4} M, respectively.

DPH. A sample (0.025 mL) of a stock solution of DPH in ethanol (5 × 10^{-2} M) was brought into a test tube. The ethanol was removed under a stream of nitrogen, and an unpolymerized or polymerized vesicle dispersion (0.05 mL) and 1.95 mL of water were added. The mixtures were vortexed for 30 s and shaken for 15 min with a Griffin flask shaker. The final amphiphile and probe concentrations amounted to 1.3 × 10^{-3} and 6.3 × 10^{-6} M, respectively.

Fluorescence Measurements. Excitation of ANS and NPN occurred at 375 and 343 nm, respectively. The fluorescence spectra were recorded with slit widths of 8 nm. The excitation wavelength of pyrene was 342 nm. The slit width in the excitation and emission beam were 2 and 4 nm, respectively. Fluorescence depolarization measurements were carried out as described in ref 34. A Schott BG24 broad-band filter was placed in the excitation beam. For the measurements with DPH two cut-off filters (Schott GG 395 and 420) and a 432-nm interference filter were placed in the emission beam. For the measurements with ANS a Schott GG 395 cut-off and a 375-nm interference filter were used. Linear polarization of the exciting light was obtained with a Glan-Thompson prism. The fluorescence anisotropy (r) was calculated by using the equation[8]

$$r = [I_{VV} - (I_{HV}/I_{HH})I_{VH}]/[I_{VV} + 2(I_{HV}/I_{HH})I_{VH}]$$

Acknowledgment. This research was supported by The Netherlands Foundation for Chemical Research (SON) with financial aid from The Netherlands Organization for the Advancement of Pure Research (ZWO). We thank M. van Gurp and H. van Langen for their assistance with the depolarization experiments and Dr. J. C. van Miltenburg for carrying out the DSC measurements.

Registry No. **1**, 103470-73-1; **1p**, 106906-21-2; **2**, 103470-74-2; **2p**, 106906-22-3; **3**, 103470-76-4; **3p**, 106906-24-5; **4**, 103470-77-5; **4p**, 106906-25-6; **5**, 70755-47-4; **6**, 3026-69-5; **7p**, 74891-05-7; **9**, 2644-64-6; **10a**, 85850-56-2; **10b**, 106929-91-3; **11a**, 85850-57-3; **10c**, 106929-93-5; **11b**, 106947-07-3; **11c**, 106929-92-4; **11d**, 106929-94-6; $(H_3C)_2N(CH_2)_{15}CH_3$, 112-69-6; $Br(CH_2)_{15}CH_3$, 112-82-3; $(H_3C)_2N(CH_2)_{17}CH_3$, 124-28-7; $Br(CH_2)_{17}CH_3$, 112-89-0; 4-OHCNHCH$(CH_3)CO_2C_6H_4NO_2$, 61167-49-5; 4-OHCNHCH$(CH(CH_3)_2)CO_2C_6H_4NO_2$, 106929-89-9; 4-OHCNHCH$((CH_2)_3CH_3)CO_2C_6H_4NO_2$, 106929-90-2; $HO(CH_2)_{11}Br$, 1611-56-9.

References and Notes

(1) (a) Laboratory of Organic Chemistry. (b) Institute of Molecular Biology.

(2) Fendler, J. H. *Membrane Mimetic Chemistry*; Wiley: New York, 1982.

(3) Calvin, M. *Acc. Chem. Res.* **1978**, *11*, 369–374. Whitten, D. G.; Russel, J. C.; Schmehl, R. H. *Tetrahedron* **1982**, *38*, 2455–2487.

(4) Bearn, A. G., Ed. *Better Therapy with Existing Drugs: New Uses and Delivery Systems.* Medical Advisory Council Plenary Session; Merck, Sharp and Dohme Int.: Rahway, NJ, 1981.

(5) Van Esch, J.; Roks, M. F. M.; Nolte, R. J. M. *J. Am. Chem. Soc.* **1986**, *108*, 6093–6094. Fuhrhop, J. H.; Malhieu, J. *Angew. Chem.* **1984**, *96*, 124–137. Tricot, Y.-M.; Fendler, J. H. *J. Am. Chem. Soc.* **1984**, *106*, 7359–7366.

(6) (a) Johnston, D. S.; Sanghera, S.; Pons, M.; Chapman, D. *Biochim. Biophys. Acta* **1980**, *602*, 57–69. (b) Hupfer, B.; Ringsdorf, H.; Schupp, H. *Chem. Phys. Lipids* **1984**, *33*, 355–374. (c) Dorn, K.; Klingbiel, R. T.; Specht, D. P.; Tyminski, P. N.; Ringsdorf, H.; O'Brien, D. F. *J. Am. Chem. Soc.* **1984**, *106*, 1627–1633. (d) Regen, S. L.; Czech, B.; Singh, A. *J. Am. Chem. Soc.* **1980**, *102*, 6638–6640. (e) Regen, S. L.; Singh, A.; Oehme, G.; Singh, M. *J. Am. Chem. Soc.* **1982**, *104*, 791–795. (f) Tundo, P.; Kippenberger, D. J.; Klahn, P. L.; Prieto, N. E.; Jao, T.-C.; Fendler, J. H. *J. Am. Chem. Soc.* **1982**, *104*, 456–461. (g) Babilis, D.; Dais, P.; Margaritis, C. H.; Paleos, C. H. *J. Polym. Sci., Polym. Chem. Ed.* **1985**, *23*, 1089–1098. (h) Samuel, N. K. P.; Singh, M.; Yamaguchi, K.; Regen, S. L. *J. Am. Chem. Soc.* **1985**, *107*, 42–47. (i) Neumann, R.; Ringsdorf, H. *J. Am. Chem. Soc.* **1986**, *108*, 487–490. (j) Roks, M. F. M.; Visser, H. G. J.; Zwikker, J. W.; Verkleij, A. J.; Nolte, R. J. M. *J. Am. Chem. Soc.* **1983**, *105*, 4507–4510.

(7) (a) Azzi, A. *Methods Enzymol.* **1974**, *32*, 234–246. (b) Waggoner, A. *Enzymes Biol. Membr.* **1976**, *1*, 119–137. (c) Slavik, J. *Biochim. Biophys. Acta* **1982**, *694*, 1–25. (d) Radda, G. K. *Curr. Top. Bioenerg.* **1971**, *4*, 81–126. (e) Haynes, D. H.; Staerk, H. *J. Membr. Biol.* **1974**, *17*, 313–340. (f) Radda, G. K.; Vanderkooi, J. *Biochim. Biophys. Acta* **1972**, *265*, 509–549.

(8) For a review, see: Wehry, E. L., Ed. *Modern Fluorescence Spectroscopy*; Heyden: London, 1976; Vol. II.

(9) (a) Lukac, S. *J. Am. Chem. Soc.* **1984**, *106*, 4386–4392. (b) Suddaby, B. R.; Brown, P. E.; Russel, J. C.; Whitten, D. G. *J. Am. Chem. Soc.* **1985**, *107*, 5609–5617. (c) Moss, R. A.; Swarup, S.; Wilk, B.; Hendrickson, T. F. *Tetrahedron Lett.* **1985**, *26*, 4827–4830. (d) Moss, R. A.; Hendrickson, T. F.; Swarup, S.; Hui, Y.; Marhy, L.; Breslauer, K. J. *Tetrahedron Lett.* **1984**, *25*, 4063–4066. (e) Rupert, L. A. M.; Hoekstra, D.; Engberts, J. B. F. N. *J. Am. Chem. Soc.* **1984**, *107*, 2628–2631. (f) Kunitake, T.; Kimizaka, N.; Higashi, N.; Nakashima, N. *J. Am. Chem. Soc.* **1984**, *106*, 1978–1983. (g) Kunitake, T.; Higashi, N. *J. Am. Chem. Soc.* **1985**, *107*, 692–696.

(10) Nome, F.; Reed, W.; Politi, M.; Tundo, P.; Fendler, J. H. *J. Am. Chem. Soc.* **1984**, *106*, 8086–8093.

(11) Bodanzky, M.; Klausner, Y. S.; Ondetti, M. A. *Peptide Synthesis*; Wiley: New York, 1976.

(12) Böhme, H.; Fuchs, G. *Chem. Ber.* **1970**, *103*, 2775–2779.

(13) (a) Bangham, A. D.; De Gier, J.; Greville, G. D. *Chem. Phys. Lipids* **1967**, *1*, 225–246. (b) Blok, M. C.; Van Deenen, L. L. M.; De Gier, J. *Biochem. Biophys. Acta* **1976**, *433*, 1–12.

(14) (a) Drenth, W.; Nolte, R. J. M. *Acc. Chem. Res.* **1979**, *12*, 30–35. (b) Van Beijnen, A. J. M.; Nolte, R. J. M.; Naaktgeboren, A. J.; Zwikker, J. W.; Drenth, W.; Hezemans, A. M. F. *Macromolecules* **1983**, *16*, 1679.

(15) The intramolecular charge-transfer processes of NPN and ANS can best be compared to a solvent polarity parameter based on a similar intramolecular charge-transfer process, e.g., the $E_T(30)$ parameter. For a discussion, see: Kosower, E. M.; Dodiuk, H.; Kanety, H. *J. Am. Chem. Soc.* **1978**, *100*, 4179–4187 and references cited therein.

(16) Radda, G. K. *Biochem. J.* **1971**, *122*, 358–396.

(17) (a) Pownall, H. J.; Smith, L. C. *J. Am. Chem. Soc.* **1973**, *95*, 3136–3140. (b) Soutar, A. K.; Pownall, H. J.; Hu, A. S.; Smith, L. C. *Biochemistry* **1974**, *13*, 2828–2836. (c) Galla, H. J.; Sackman, E. *Biochim. Biophys. Acta* **1974**, *339*, 103–115. (d) Vanderkooij, J. M.; Callis, J. B. *Biochemistry* **1974**, *13*, 4000–4006.

(18) For a review on this technique, see: Shinitzky, M.; Barenholz, Y. *Biochim. Biophys. Acta* **1978**, *515*, 367–394.

(19) One helical turn of the polymer chain (four repeating units) corresponds to a length of 4 Å. From the average degree of polymerization the number of helical turns can be calculated, and from this number the average chain length can be determined; see ref 14.

(20) Branton, D. *Proc. Natl. Acad. Sci. U.S.A.* **1966**, *55*, 1048–1056. Pinto da Silva, P.; Branton, D. *J. Cell. Biol.* **1970**, *45*, 598–605.

(21) For small polymerized vesicles (probably not the large ones) a third way of fracturing is conceivable, viz., along the vesicle–water interface. Whether such a splitting actually occurs cannot be decided from the present electron micrographs.

(22) NMR line-width experiments show additional phase transitions of the vesicle bilayers at 30 °C. In our previous paper[6] we erroneously took these transitions for the main transitions.

(23) Kumano, A.; Kajiyama, T.; Takayanagi, M.; Kunitake, T.; Okamota, Y. *Ber. Bunsenges. Phys. Chem.* **1984**, *88*, 1216–1222.

(24) Kusumi, A.; Singh, M.; Tirrell, D. A.; Oehme, G.; Singh, A.; Samuel, N. K. P.; Hyde, J. S.; Regen, S. L. *J. Am. Chem. Soc.* **1983**, *105*, 2975–2980.

(25) Wagner, N.; Dose, K.; Koch, H.; Ringsdorf, H. *FEBS Lett.* **1981**, *132*, 313–318.

(26) Trauble, H.; Overath, P. *Biochim. Biophys. Acta* **1973**, *307*, 491–512.

(27) (a) Demchenko, A. P. *J. Mol. Struct.* **1984**, *114*, 45–48. (b) Demchenko, A. P. *Biophys. Chem.* **1982**, *15*, 101–109.

(28) (a) Colley, C. M.; Metcalfe, J. C. *FEBS Lett.* **1972**, *24*, 241–246. (b) Lesslauer, W.; Cain, J.; Blasie, J. K. *Biochim. Biophys. Acta* **1971**, *241*, 547–566.

(29) The solvent polarities of the head group region and the inner part of the vesicles, as measured by ANS and NPN, respectively, do not lie on the same polarity scale (Figure 7). The reason for this phenomenon is not clear yet. It could be that the fluorescence behavior of ANS is somehow influenced by the positive and negative charges of the quaternary ammonium functions and the Br^- ions. In separate experiments, however, we found that adding benzyltriethylammonium bromide to solutions of ANS in dioxane–water mixtures did not change the position of the fluorescence maximum.
(30) (a) Forster, Th.; Rokos, K. *Chem. Phys. Lett.* **1967**, *1*, 279–280. (b) Robinson, G. W.; Robbins, R. J.; Fleming, G. R.; Morris, J. M.; Knight, A. E. W.; Morrison, R. J. S. *J. Am. Chem. Soc.* **1978**, *100*, 7145–7150.
(31) Roks, M. F. M., unpublished results.
(32) Nagamura, T.; Mihara, S.; Okahata, Y.; Kunitake, T.; Matsuo, T. *Ber. Bunsenges. Phys. Chem.* **1978**, *82*, 1093–1098.
(33) Galla, H. J.; Sackman, E. *Ber. Bunsenges. Phys. Chem.* **1974**, *78*, 949–953.
(34) Goedheer, J. C. *Photobiochem. Photobiophys.* **1984**, *7*, 91–101.
(35) Ververgaert, P. H. J. Th.; Elbers, P. F.; Luitingh, A. J.; Van de Berg, N. J. *Cytobiology* **1972**, *6*, 86–96.
(36) Schore, N. E.; Turro, N. J. *J. Am. Chem. Soc.* **1975**, *97*, 2488–2496.
(37) Westphal, O.; Jerchel, D. *Chem. Ber.* **1940**, *73*, 1002–1011.
(38) Rothe, M.; Kunitz, F. W. *Justus Liebigs Ann. Chem.* **1957**, *609*, 88–102.
(39) For a discussion, see: Bolikal, D.; Regen, S. L. *Macromolecules* **1984**, *17*, 1287–1289.

Polymerization of Liposomes Composed of Diene-Containing Lipids by UV and Radical Initiators: Evidence for the Different Chemical Environment of Diene Groups on 1- and 2-Acyl Chains

Hiroyuki Ohno, Yoshitaka Ogata, and Eishun Tsuchida*

Department of Polymer Chemistry, Waseda University, Tokyo 160, Japan.
Received March 7, 1986

ABSTRACT: 1,2-dioctadecadienoyl-3-phosphatidylcholine (DODPC), a polymerizable lipid that contains one diene group per acyl chain, was polymerized as liposomes. Polymerization was done by UV irradiation or by the addition of a radical initiator. Water-insoluble azobis(isobutyronitrile) (AIBN) and/or water-soluble azobis(2-amidinopropane) dihydrochloride (AAPD) were examined. The UV irradiation for 3 h provided a complete polymerization of DODPC liposomes. Contrary to this, polymerization by the addition of radical initiator (AIBN or AAPD) gave 50–60% polymerization conversion at 60 °C. Complete polymerization was performed by the use of AIBN and AAPD simultaneously. The polymerization conversion was also improved by the addition of AAPD to liposomes that were preliminarily polymerized by AIBN. The DODPC liposomes polymerized by both AIBN and AAPD provided the most stable polymerized liposomes. The liposomes polymerized by both AIBN and AAPD showed the least carboxyfluorescein leakage from the inner aqueous phase. The obtained results strongly suggested that the diene groups in 2-acyl chains should face the aqueous phase, and therefore polymerization was initiated by a water-soluble radical initiator (AAPD) but not by AIBN.

Introduction

Phospholipid bilayer liposomes are gathering keen interest as microcapsules for carriers of drugs or functional particles as well as models for biomembranes.[1,2] These liposomes are generally not very stable and cause aggregation and fusion. To stabilize these assembled structures polymerizable lipids were synthesized as a major component in constructing the membrane. The physicochemical properties of the polymerized liposomes have been collected vigorously in this decade.[1-12] Several unique liposomes were also prepared by polymerization, such as corked liposomes,[13] ghost liposomes,[14] skeletonized liposomes,[15] etc. Most of the polymerizations have been performed by UV irradiation because of its convenience. Although polymerization is one of the most potent techniques in principle, the actual polymerized systems thus prepared have several problems such as distortion of the assembled structure and formation of clefts or cracks in the membranes that were induced by polymerization.[16,17] In this paper, diene-type monomeric lipids were polymerized as liposomes by UV irradiation or by radical initiators to compare the characteristics of the obtained polymeric liposomes.

Experimental Section

Materials. 1,2-di(2,4-octadecadienoyl)-3-phosphatidylcholine (DODPC) was purchased form Nippon Oil & Fats Co. Ltd. This was characterized by thin-layer chromatography (Merck, silica gel plates) with chloroform/methanol/water (65/35/5, by vol) as solvent before use.[17] DODPC showed a single spot with an R_f value of 0.3, similar to that of 1,2-distearoyl-3-phosphatidylcholine (special grade, Sigma).

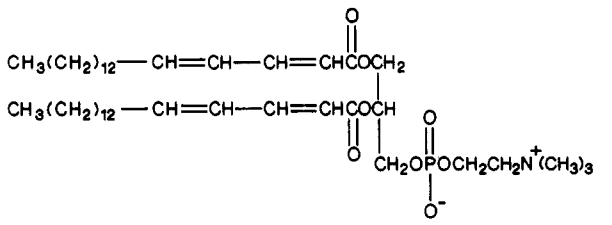

DODPC

Azobis(isobutyronitrile) (AIBN) and azobis(2-amidinopropane) dihydrochloride (AAPD) were purchased from Tokyo Kasei Co. Ltd. AIBN and AAPD were purified twice by recrystallization from methanol and water, respectively.

Triton X-100, polyethylene glycol mono-*p*-octylphenyl ether ($HO(CH_2CH_2O)_{10}C_6H_4C_8H_{17}$), was purchased from Tokyo Kasei Co. Ltd. and was used without further purification. Fluorescent grade 5(6)-carboxyfluorescein (CF) was purchased from Kodak Co. Ltd.

Methods. A total of 0.200 g of lipids was dissolved in dehydrated chloroform and was slowly evaporated in a rotated sample tube to prepare a thin lipid film on the inner surface of the tube. A degassed phosphate buffer solution (pH 7.0, 20 mL) was then added to the tube. The liposome suspension (1.0 wt %) was prepared by sonication (Tomy Seiko UR-200P) at 60 W for 10 min under a nitrogen atmosphere.[17] The freshly prepared liposome suspensions were incubated at 4 °C overnight to minimize

0024-9297/87/2220-0929$01.50/0